Origins of Stereoselectivity in the Corey–Chaykovsky Reaction. Insights from Quantum Chemistry

Mika K. Lindvall and Ari M. P. Koskinen*

Department of Chemistry, University of Oulu, P.O. Box 3000, FIN-90401 Oulu, Finland

Received September 17, 1998

Reaction pathways of the Corey–Chaykovsky epoxidation reaction have been compared quantum chemically. Of the concerted, torsional rotation and anti addition pathways the latter two were found to be favored both in the gas phase and in CH_2Cl_2 in a model system. Several theoretically previously uncharacterized stationary points were located, and selective solvent effects were observed. On the anti addition pathway the C–C bond formation transition state **A**, suitably substituted to allow comparison with published experimental data, was able to predict both the absolute stereochemistry of the main product and, qualitatively, the distribution of its other stereoisomers. The quantum chemical protocol reported here is useful in designing new sulfides for the Corey–Chaykovsky reaction.

Background

Recent stereoselective and catalytic versions of the Corey–Chaykovsky reaction[1] have provided the synthetic chemist with a viable route from aldehydes to optically pure epoxides.[2] While optically pure sulfides act as the source of chirality, the exact mechanism of the chirality transfer is not known. Furthermore, experimental and theoretical observations consistent with two mechanistic extremes have been reported.[3] The nature and structure of the transition state determining the stereoselectivity is strategically important in the rational design of new sulfides for the Corey–Chaykovsky reaction. In connection with our experimental program of developing new enantioselective sulfides for this reaction, we decided to study the origins of stereoselectivity in this reaction by molecular modeling. Particular emphasis was placed on studying substituent and medium effects relevant to the conditions in the catalytic version of the reaction.[4]

The intermediates and transition states of the Corey–Chaykovsky reaction derived from previously reported experimental[3,5,6] and theoretical[3,7] evidence have been collected in Scheme 1. The suggested pathways connecting the intermediates and transition states are based on experimental data and findings reported here. We have assigned them as anti addition, torsional rotation, and concerted pathways. Previous ab initio calculations have

been able to locate all other stationary points but not **B**, **C**, **D**, and **F**.[3,7]

Although less frequently used to account for the mechanism of the Corey–Chaykovsky reaction, the concerted pathway has been convincingly demonstrated experimentally.[3] A substituted oxathietane **E**, isolated and characterized by NMR and X-ray diffraction, yields epoxides with retention of configuration after oxidation and thermolysis, strongly suggesting passage via transition state **G**. Reduced stereoselectivity is observed on thermolysis in the presence of lithium salts, implying that the concerted pathway should be considered a salt-free Corey–Chaykovsky reaction. Unlike in the catalytic version,[4] the sulfur atom has a higher oxidation state and the substrate contains several trifluoromethyl substituents.

In the catalytic conditions, however, the reaction of sulfonium benzylides with aldehydes has been proposed to proceed via the anti addition pathway.[4] Aggarwal et al. combine knowledge of the structure and absolute stereochemistry of the chiral sulfide catalyst, of the resulting less-hindered direction of approach of the aldehyde and of the assumed ylide conformational preference to account for the absolute stereochemistry of the major enantiomer of *trans*-stilbene oxide formed in one of the reactions examined (Scheme 2). The catalytic Corey–Chaykovsky reaction is typically performed in CH_2Cl_2 in the presence of small amounts of transition metal complexes to catalyze the formation of sulfonium ylides from diazo compounds.

Stereochemical consequences of the different pathways are illustrated in Scheme 1. Starting materials can initially combine via transition states **A** or **D**. Assuming that the ylide preferentially adopts the same conformation (for a discussion of ylide conformations, see Results) in both **A** and **D** and that in both TSs the trans approach relative to the substituents R^1 and R^2 is preferred, the anti addition pathway and the concerted pathway lead to enantiomeric products. In the torsional rotation pathway the S–O interaction[8] in **E** is broken, followed by rotation of the SCCO torsion angle and product formation via **B** and **C**. The torsional rotation pathway leads to cis epoxides.

* Corresponding author. Phone: +358 8 553 1630, fax +358 8 553 1629, e-mail: Ari.Koskinen@oulu.fi.

(1) Corey, E. J.; Chaykovsky, M. *J. Am. Chem. Soc.* **1965**, *87*, 1353–1364.

(2) (a) For an excellent recent review, see Li, A.-H.; Dai, L.-X.; Aggarwal, V. K. *Chem. Rev.* **1997**, *97*, 2341–2372. More recent examples: (b) Julienne, K.; Metzner, P.; Henryon, V.; Greiner, A. *J. Org. Chem.* **1998**, *63*, 4532–4534. (c) Aggarwal, V. K.; Bell, L.; Coogan, M. P.; Jubault, P. *J. Chem. Soc., Perkin Trans. 1* **1998**, 2037–2042. (d) Aggarwal, V. K.; Blackburn, P.; Fieldhouse, R.; Jones, R. V. H. *Tetrahedron Lett.* **1998**, *39*, 8517–8520.

(3) Kawashima, T.; Ohno, F.; Okazaki, R.; Ikeda, H.; Inagaki, S. *J. Am. Chem. Soc.* **1996**, *118*, 12455–12456.
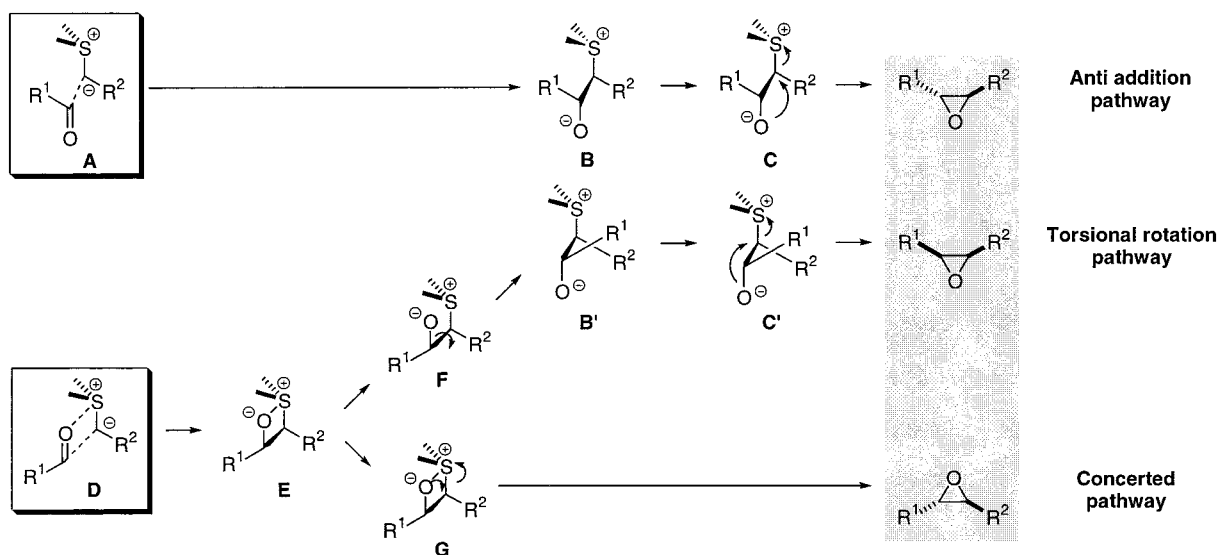
(4) Aggarwal, V. K.; Ford, J. G.; Thompson, A.; Jones, R. V. H.; Standen, M. C. H. *J. Am. Chem. Soc.* **1996**, *118*, 7004–7005.

(5) Aggarwal, V. K.; Ford, J. G.; Fonquerna, S.; Adams, H.; Jones, R. V. H.; Fieldhouse, R. *J. Am. Chem. Soc.* **1998**, *120*, 8328–8339.
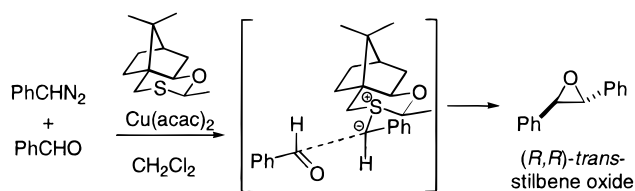
(6) Solladié-Cavallo, A.; Diep-Vohuule, A. *J. Org. Chem.* **1995**, *60*, 3494–3498.

(7) Volantron, F.; Eisenstein, O. *J. Am. Chem. Soc.* **1987**, *109*, 1–14.

Scheme 1

Scheme 2

We have used quantum chemical calculations to chart the contributions to stereoselectivity from the mechanistic alternatives, conformations, and directional selectivity, using a consistent theoretical treatment and including substituent and solvation effects where possible. Particular emphasis was placed on studying substituent and medium effects relevant to the conditions in the catalytic version of the reaction.[4] Our strategy was to first study the reaction in the gas phase and in CH_2Cl_2 with simple model molecules to enumerate the possible intermediates and transition states. For this purpose, the reaction between dimethylsulfonium methylide **6** and formaldehyde **7** was examined (Scheme 3). Low energy transition states from the model reaction were chosen for further studies. Substituents allowing comparison with experiment were used to evaluate conformational preferences and facial selectivity in these systems. We focused on the formation of stilbene oxide since the majority of sulfides used in the Corey–Chaykovsky reaction have been examined in stilbene oxide formation. The work resulted in a transition state model capable of accounting for the experimentally observed stereoselectivity in stilbene oxide formation, in terms of the relative energies of the transition states.

Computational Details

General. Gaussian94 was used for all calculations.[9] The default convergence criteria were used in all optimizations. All stationary points on the B3LYP/6-31+G* and HF/6-31G* energy surfaces and those obtained from unfrozen optimization at the HF/3-21G* level were characterized by normal-mode analysis. Zero-point energies (ZPE) of the HF/6-31G* geometries[10] were scaled by 0.9135 and those[11] of HF/3-21G* by 0.9167, while those of B3LYP/6-31G* were left unscaled.[12]

Solvation energies in dichloromethane for the gas-phase geometries were calculated using the continuum solvation model of Tomasi[13–15] with a charge isodensity defined cavity shape (as implemented in Gaussian94, IPCM option). A dielectric constant of 8.9 for CH_2Cl_2 and charge density value[13] of 0.0004 e B^{-3} were employed in the solvation calculations.

Basis Set and Electron Correlation Effects. Sulfonium ylide geometries have been previously reported not to be sensitive to electron correlation or to the basis set.[16] We optimized the geometry of dimethylsulfonium dicyanomethylide (Cambridge Structural Database (CSD) code MSMNIT) with AM1, PM3, HF/3-21G*, HF/6-31G*, and B3LYP/6-31G*, all previously untested in this case. HF/3-21G* provided a good and HF/6-31G* and B3LYP/6-31G* an excellent account of the geometry, thus confirming the previous observations. With semistabilized ylides, such as benzylidene ylides studied here, HF/3-21G* provides geometries comparable to the higher levels of treatment whereas with unstabilized ylides, such as **6**, HF/3-21G* is not sufficient.

Transition state geometries proved more sensitive to the basis sets. **3** can be located with HF/3-21G* and B3LYP/6-31+G* (HF/6-31G* not tested), **5** with HF/3-21G*, HF/6-31G*, and B3LYP/6-31+G*, **9** with HF/6-31G* only, and **10** with PM3, HF/3-21G*, and HF/6-31G*. Several additional methods were tested for their ability to locate **8** (Figure 1). HF/3-21+G* and HF/6-31G* proved the minimal levels, and the value for the C–C bond turned out not to be well defined in **8**.

(8) Although the term oxathietane implies a S–O bond, there is controversy about the nature of this bond (see ref 7 and the references cited therein), and a weakly bonded situation has been suggested. Our computational results are consistent with such interpretation, and we prefer the term S–O interaction.

(9) Frisch, M. J.; Trucks, G. W.; Schlegel, H. B.; Gill, P. M. W.; Johnson, B. G.; Robb, M. A.; Cheeseman, J. R.; Keith, T.; Petersson, G. A.; Montgomery, J. A.; Raghavachari, K.; Al-Laham, M. A.; Zakrzewski, V. G.; J. V. Ortiz, J. B. F.; Cioslowski, J.; Stefanov, B. B.; Nanayakkara, A.; Challacombe, M.; Peng, C. Y.; Ayala, P. Y.; Chen, W.; Wong, M. W.; Andres, J. L.; Replogle, E. S.; Gomperts, R.; Martin, R. L.; Fox, D. J.; Binkley, J. S.; Defrees, D. J.; Baker, J.; Stewart, J. P.; Head-Gordon, M.; Gonzalez, C.; Pople, J. A. *Gaussian94*; Gaussian, Inc.: Pittsburgh, PA, 1995.

(10) Scott, A. P.; Radom, L. *J. Phys. Chem.* **1996**, *100*, 16502–16513.

(11) Ochterski, J. W.; Petersson, G. A.; J. A. Montgomery, J. *J. Chem. Phys.* **1996**, *104*, 2598–2619.

(12) Brandt, P.; Norrby, P.-O.; Martin, I.; Rein, T. *J. Org. Chem.* **1998**, *63*, 1280–1289.

(13) Foresman, J. B.; Keith, T. A.; Wiberg, K. B.; Snoonian, J.; Frisch, M. J. *J. Phys. Chem.* **1996**, *100*, 16098–16104.

(14) Tomasi, J.; Maurizio, P. *Chem. Rev.* **1994**, *94*, 2027–2094.

(15) Miertus, S.; Scrocco, E.; Tomasi, J. *Chem. Phys.* **1981**, *55*, 117–129.

(16) Shimizu, T.; Matsuhisa, A.; Kamigata, N.; Ikuta, S. *J. Chem. Soc., Perkin Trans. 2* **1995**, 1805–1808.

Scheme 3.   The Model Reaction Used in Quantum Chemical Studies of the Alternative Reaction Mechanisms
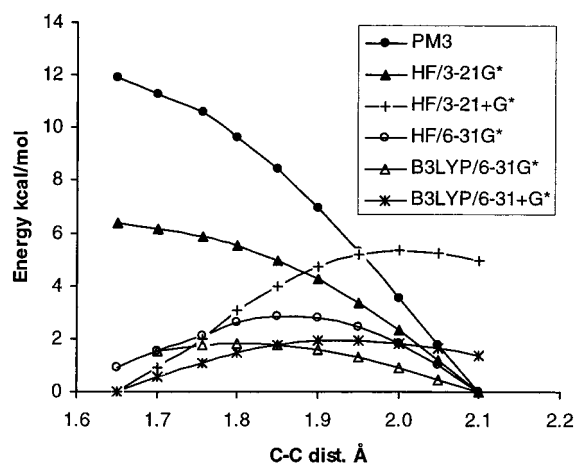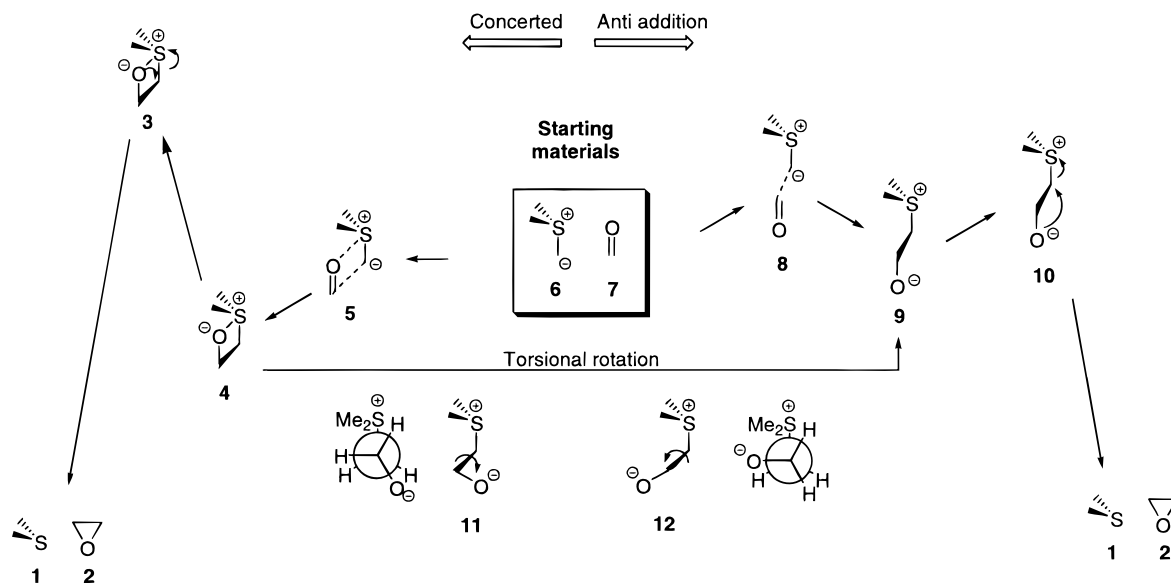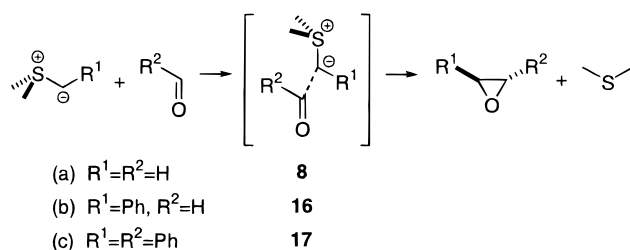

Figure 1. Energy as the function of the length of the forming C−C bond in **8**. The forming C−C bond was frozen to specific lengths at 0.1 Å increments and all other degrees of freedom were relaxed, except the SCCO angle which was frozen to 180° at every increment.

Scheme 4.   The Isodesmic Reaction Series

  (a) R^1=R^2=H   **8**
  (b) R^1=Ph, R^2=H   **16**
  (c) R^1=R^2=Ph   **17**

Diffuse functions were avoided in geometry determinations with the larger systems due to the added computational cost and slower convergence. However, diffuse functions were included in calculating final energies. The heat of reaction and activation energy calculated for reaction a (Scheme 4) at the B3LYP/6-31+G* and B3LYP/6-31+G*//HF/6-31G* levels reveal a maximum error of 0.6 kcal/mol due to absence of diffuse functions in geometry determination. Since these are absolute energies, smaller errors are expected in relative energies, such as relative activation energies between stereoisomeric transition states.

Results

Ylide Structure. Both HF/6-31G* and B3LYP/6-31+G* predict a pyramidal ylide carbon and sulfur in dimethylsulfonium methylide **6**, suggesting the ylide carbon is very anionic in nature. However, the introduction of a phenyl group, yielding benzylidene ylides, leads to a planar ylide carbon. The filled p orbital of the sp^2-hybridized ylide carbon is perpendicular to the plane of the aromatic ring and the lone pair of the sp^3-hybridized sulfur. The overall geometry (Figure 2) is similar to that of dimethylsulfonium fluoren-9-ide decuded from NMR data[17] and to those of highly stabilized ylides, such as that of dimethylsulfonium dicyanomethylide (CSD code MSMNIT) determined by X-ray. The ylide bond is shortened and the ylide carbon−substituent bond elongated in dimethylsulfonium benzylide **10** compared to the corresponding bonds in MSMNIT.

Ylide Conformation. Due to rotation about the ylide bond, **13** can adopt two conformations where the phenyl group is either syn or anti relative to the sulfur electron pair (Figure 2). Although the anti conformer seems sterically less favorable, the close contact between the phenyl hydrogen and the methyl hydrogens can be alleviated by the increased S$^+$−C$^-$−C$_{ar}$ angle and more planar sulfur atom. Furthermore, examination of electron density isosurfaces suggests there is also a close contact in the syn conformation, between the lone pair of sulfur and the phenyl hydrogen. Thus, both conformers can be sterically crowded and approximately equal in energy. The geometry differences are not sensitive to the level of theory as HF/3-21G*, HF/6-31G*, and B3LYP/6-31G* all yield similar trends between the conformer pair.

The relative energies of sulfonium benzylide conformers depend on the level of theory and the structure of the parent sulfide (Table 1). Our best estimate for **13** predicts that the anti conformer is favored by 0.4 kcal/mol in the gas phase and the syn conformer by 0.3 kcal/mol in CH$_2$Cl$_2$. Although the higher level gas phase and solvation energies are not available for **15**, the gas-phase

(17) Aggarwal, V. K.; Schade, S.; Taylor, B. *J. Chem. Soc., Perkin Trans. 1* **1997**, 2811−2813.
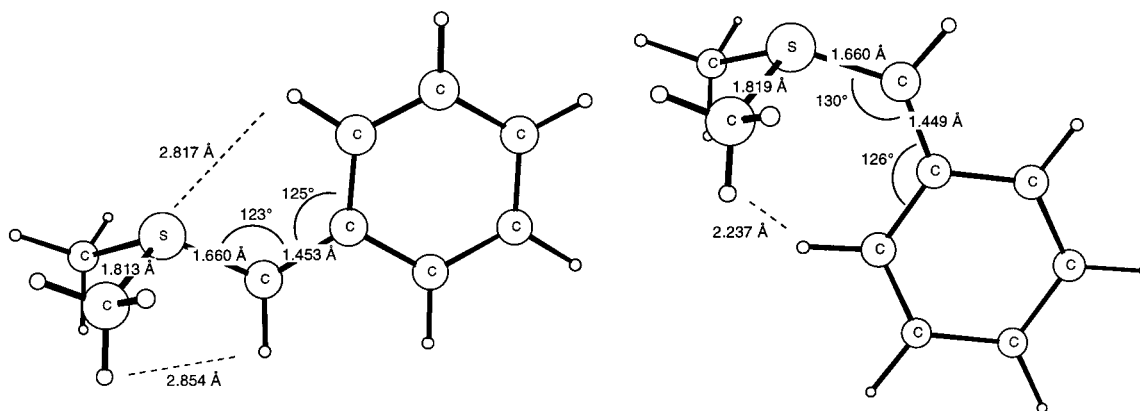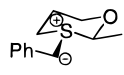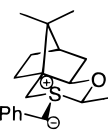
Figure 2. Geometries of the syn (top) and anti (bottom) conformations of dimethylsulfonium benzylide **13** at the HF/6-31G* level.

Table 1. The Energy (in kcal/mol) of the Syn Conformer Relative to the Anti Conformer of Various Sulfonium Benzylides

level of theory	13	14	15
HF/3-21G*	0.7	0.1	0.1
B3LYP/6-31+G*//HF/3-21G*	0.6	0.0	0.0
+$\Delta\Delta E_{solv}$ (CH$_2$Cl$_2$)	−0.2	0.8	
B3LYP/6-31+G*//HF/6-31G*	0.6		
+ZPE	0.4		
+ZPE + $\Delta\Delta E_{solv}$ (CH$_2$Cl$_2$)	−0.3		

Table 2. The Relative Energies (in kcal/mol) of the Stationary Points (Scheme 3) at the B3LYP/6-31+G* and B3LYP/6-31+G*//HF/6-31G* (9 and 10) Levels. Selected HF/6-31G* Energies Included To Reveal the Nature of 9 and 10. ZPE Included in All Energy Values

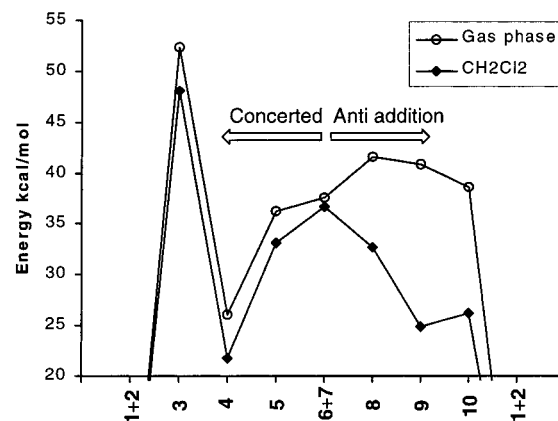| point	gas phase HF/6-31G*	gas phase	CH$_2$Cl$_2$
3		52.4	48.1
4		26.1	21.8
5		36.3	33.2
11		43.7	28.3
12		42.0	27.4
6 + 7	48.3	37.5	36.6
8	62.2	41.6	32.7
9	60.8	40.8	24.9
10	61.4	38.6	26.3
1 + 2	0.0	0.0	0.0

Figure 3. The energies of the concerted and anti addition pathway stationary points relative to **1** + **2** (0 kcal/mol, not shown). ZPE included in all energies.

data suggest that the results with **14** can be safely extrapolated to **15**, a postulated intermediate in the published reaction.[4] Consequently, in the cyclic sulfonium benzylides **14** and **15** the syn and anti conformations have equal energies in the gas phase but the anti conformer is preferred by 0.8 kcal/mol in CH$_2$Cl$_2$. ZPE contribution is expected to be small.

There is an interesting opposite solvation energy trend in **13** and **14**. Because much of the charge density in sulfonium benzylides is delocalized into the phenyl ring, the solvation energies are sensitive to solvent accessible surface areas. While the syn conformer has a higher dipole moment in both **13** and **14**, the syn conformer has a larger solvent accessible surface in **13** and a smaller in **14**, due to the shielding methyl group in **14**. Further geometry and energy determinations for **13** at various levels of theory (see Supporting Information) provide an energy range of 0.5−1.4 kcal/mol (without ZPE) for the anti conformer preference in the gas phase. Overall, the conformational equilibrium does not seem very sensitive to the theoretical treatment, with HF/3-21G* providing reasonable consensus estimates.

Stationary Points of the Model Reaction. The Corey−Chaykovsky reaction depicted in Scheme 3 was studied both in the gas phase and in CH$_2$Cl$_2$ using the model molecules illustrated in Scheme 3. The three alternative pathways in the context of the model reaction are described in detail below. The stationary points and their energies are listed in Table 2 and plotted in Figure 3 (**11** and **12** excluded from the plot). Solvation energies were calculated for the gas-phase geometries. Point **6** + **7** corresponds to the combined energy of the starting

materials and point **1** + **2** to the combined energy of the products, both at infinite separation. Two additional minima could be located, oxathietane **4** and anti betaine **9**. Six transition states were found, **3**, **5**, **8**, **10**, **11**, and **12**. Structures **9** and **10** could be located as stationary points at the HF/6-31G* level but not at the B3LYP/6-31+G* level.

In the reaction energy profile in Figure 3 the starting materials **6** + **7** have a high energy relative to the transition states **5** and **8**. Thus, in the gas phase **5** is lower in energy than **6** + **7**, while in CH$_2$Cl$_2$ this is true for both **5** and **8**. The apparent lack of energy barriers is likely to be a special feature of our model reaction and modeling protocol, and the issue is addressed in Discus-

Table 3. The Geometries of Selected Stationary Points at the B3LYP/6-31+G* Level (except 9 and 10 at the HF/6-31G* Level). Numbering System from Figure 4

coordinate	3	4	5	8	9	10	11	12
S−C (Å) (1-2)	1.835	1.882	1.857	1.856	1.804	1.806	1.838	1.835
S−C (Å) (2-3)	1.822	1.826	1.822	1.824	1.803	1.804	1.822	1.825
S−C (Å) (2-4)	2.495	1.851	1.734	1.769	1.861	2.046	1.819	1.857
S−O (Å) (2-6)	2.782	2.202	3.465					
C−C (Å) (4-5)	1.470	1.540	2.160	1.936	1.591	1.536	1.665	1.616
C−O (Å) (5-6)	1.382	1.378	1.249	1.259	1.290	1.309	1.295	1.311
CCO (deg) (4-5-6)	95	102	114	105	105	97	111	108
SCCO (deg) (2-4-5-6)	38	−28	−51	175	176	180	114	−137
CSCC (deg) (3-2-4-5)	41	92	58	52	59	60	77	72
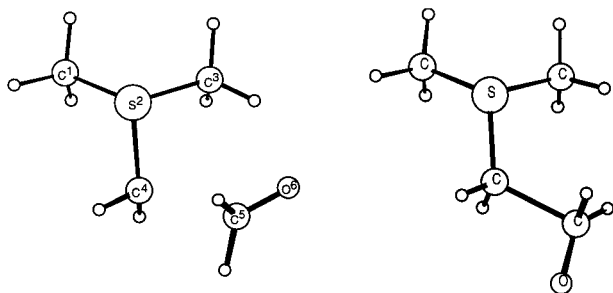
Figure 4. Transition states **5** (left) and **8** (right). Selected coordinates in Table 3.

sion. However, our theoretical protocol yields energy barriers relative to the starting materials both in the gas phase and in CH_2Cl_2 with the semistabilized sulfonium benzylides (see below).

The Concerted Pathway. Passage from starting materials to products via **5**, **4**, and **3** constitutes the concerted reaction pathway (Figure 3, left part). Characteristic to this pathway is the concerted nature of the epoxide formation TS **3**. The first step in this pathway is the combination of the starting materials via TS **5** to yield oxathietane **4**. The geometries of **5** and **4** are described in Table 3. The imaginary frequency in **5** corresponds to the carbon−carbon bond formation between C4 and C5. We attempted to locate another conformer of **5** where SCCO was +60°, but the optimization converged to the geometry already described.

The C−C bond between the carbonyl and ylide carbons is already present in oxathietane **4**. An increase in the S−C distance (Table 3, dist. 2−4) and in the SCCO torsion angle and reduction of the CCO angle lead to **3**. In this TS the imaginary frequency corresponds to the simultaneous breaking of the S−C bond and epoxide ring closure. Solvation lowers the relative energies of **5**, **4**, and **3** by 3−4 kcal/mol. Energetically, passage from **4** to the products via TS **3** is unfavorable compared to the torsion rotation pathway discussed below.

The Anti Addition Pathway. Stationary points **8**, **9**, and **10** form the anti addition pathway (Figure 3, right). Here the SCCO torsion angle is ca. 180°, as opposed to approximately 0° in the concerted pathway. The imaginary frequency in TS **8** corresponds to the C−C bond formation between the carbonyl and ylide carbons (Figure 4, Table 4).

In our computational studies the number of steps from **8** to the products depends on the level of theory used. At the B3LYP/6-31+G* level, **8** leads directly to the products, as evidenced by an IRC calculation. Similar behavior has been reported at the HF/4-31G* level.[7] At the HF/6-31G* level two additional stationary points can be located. Anti betaine **9** is a shallow minimum and **10** the

Table 4. Geometric Parameters of 8, 16, and 17 (Scheme 4) at the HF/6-31G* Level

coordinate[a]	8	16	17
S−C (Å) (1-2)	1.808	1.808	1.809
S−C (Å) (2-3)	1.800	1.800	1.803
S−C (Å) (2-4)	1.790	1.810	1.838
C−C (Å) (4-5)	1.870	1.863	1.853
C−O (Å) (5-6)	1.241	1.245	1.252
C−C$_{ar}$ ylide (Å)		1.497	1.500
C−C$_{ar}$ PhCHO (Å)			1.524
CCO (deg) (4-5-6)	105	106	103
SCCO (deg) (2-4-5-6)	175	−161	−156
CSCC (deg) (3-2-4-5)	53	57	73
CCC$_{ar}$C$_{ar}$[b] ylide (deg)		6	3
CCC$_{ar}$C$_{ar}$[b] PhCHO (deg)			6

[a] Atom numbering defined in Figure 4. [b] Torsion angle defined by the two carbon atoms of the forming C−C bond and the two aromatic carbons, all in a bonded array.[32] Deviation from 90° is reported.

ring closure transition state. The imaginary frequency in **10** corresponds to simultaneous cleavage of the S−C bond and a reduction in the CCO angle to afford ring closure, without change in the C−C bond length. When the energies of **9** and **10** are calculated at the B3LYP/6-31+G* level, using the HF/6-31G* geometries, **9** and **10** do not appear to be stationary points.

Solvation has a significant effect on the energies of the anti addition pathways structures. The energies of **8**, **9**, and **10** are lowered by 9, 16, and 12 kcal/mol, respectively. Thus, **9** and **10** are likely to be stationary points at the B3LYP/6-31+G* level only in CH_2Cl_2, not in the gas phase.[18] It is possible that HF/6-31G*, due to its tendency to overestimate dipole moments,[19] approximates some aspects of solution behavior while B3LYP/6-31+G* better reproduces "real" gas-phase behavior.

The Torsional Rotation Pathway. A third pathway to the products, the torsional rotation pathway, is a hybrid of the concerted and anti addition pathways. It consists of initial combination of the starting materials via TS **5** to yield **4**. Instead of direct epoxide formation, the S−O interaction[8,20] is broken and the SCCO torsion is rotated via **11**/**12** to reach the anti addition pathway structures **9** and **10**. The structures of **11** and **12** are

(18) While the single point calculations in solvent *suggest* **9** and **10** are stationary points in solution, their nature in CH_2Cl_2 at the B3LYP/6-31+G* level cannot be *proven* without optimization in solution. Such methodology was not available to us while the majority of this work was carried out. While revising the manuscript, we had limited access to Gaussian98 and the implementation of Tomasi's continuum solvation model with gradients. Our preliminary studies with this optimization approach afford **9** as a minimum at the B3LYP/6-31+G* level, when optimized in the presence of CH_2Cl_2.

(19) Kuyper, L.; Ashton, D.; Merz, K.; Kollman, P. A. *J. Phys. Chem.* **1991**, *95*, 6661−6666.

(20) The S−O distance in **4**, 2.2 Å at the B3LYP/6-31+G* level, is relatively large for a covalent bond. Furthermore, the electron density between S and O is much lower than in the covalent bonds in **4**, as revealed by examination of electron density isosurfaces.

Table 5. The ΔE and E_a of the Reactions a, b, and c (Scheme 4) at the B3LYP/6-31+G*//HF/6-31G* Level. ZPE Included in the Energies

reaction	ΔE	ΔE in CH_2Cl_2	E_a	E_a in CH_2Cl_2
a	38.3	37.0	3.5	−5.7
b	37.2	33.7	8.5	1.4
c	30.6	29.5	14.0	10.8

described in Table 3. In both TSs, the imaginary frequency corresponds to the rotation of the SCCO torsion angle.

In the model reaction in the gas phase, the energetic cost of breaking the S–O interaction in **4** and SCCO torsional rotation to reach **11** or **12** is high (Table 2). In fact, **11** and **12** are both higher in energy than the C–C bond formation TS **8**. In CH_2Cl_2 the opposite is true, as solvation lowers the energies of **11** and **12** by 15 kcal/mol (compared to 9 kcal/mol in the case of **8**). Thus, in solution the "downhill events" in the anti addition and torsional rotation pathways are energetically equally likely, and the preferred pathway depends on the relative energetic feasibility of the transition states (**8** and **5**, respectively) where the starting materials are initially combined. In the model reaction, the anti addition pathway TS **8** is favored slightly, by 0.5 kcal/mol, over **5**.

The Effect of Phenyl Substituents on Transition State Geometry, $\Delta E_{reaction}$ and E_a. Assuming passage via the anti addition pathway, the relative effects of phenyl substitution on the transition state geometry, the energy of reaction, and the activation energy were studied systematically in an isodesmic reaction series (Scheme 4). In reaction c the formation of *trans*-stilbene was studied as trans epoxides are usually the predominant products in the Corey–Chaykovsky reactions. The C–C bond formation transition state was assumed to be responsible for the activation barrier, and the equivalent stereoisomeric forms (in a microscopic sense) of the transition state were used throughout. As a consistent level of theory is necessary for a comparative study and the system substituted with two phenyls is relatively large, HF/6-31G* was used for geometry determination and normal-mode analysis in all systems.[21] Overall, the transition state geometries (Table 4) **8** and **16** are quite similar, whereas **17** differs more from **8** and **16**. The successive introduction of phenyl groups slightly reduces the length of the forming C–C bond and the CCO angle and lengthens the cleaving S–C bond. The largest changes occur in the SCCO and CSCC torsion angles, and in **14** the reaction coordinate (C**S**CC) has to rotate significantly to avoid the bad steric contact with the Me₂S moiety (**CS**CC).

Final energies (Table 5) were calculated at the B3LYP/6-31+G*//HF/6-31G* level and the effect of CH_2Cl_2 estimated for reactions a and b. Overall, the introduction of phenyl groups raises the activation energy and lowers the energy of reaction. With the introduction of a phenyl group in the ylide, a positive absolute activation energy is observed in CH_2Cl_2.

The Stereoisomeric Transition States with 13 as the Ylide Component. The role of various stationary points in *trans*-stilbene oxide formation was further studied in a systematic fashion. Thus, transition states

Table 6. Relative Energies (in kcal/mol) of Stereoisomeric Transition States Involved in Stilbene Oxide Formation at the HF/3-21G* Level. The Torsional Rotation Pathway Is Assumed in Translating the Configurations of 18–21 to the Stereochemical Configurations of the Products

Stilbene oxide stereochemistry	(R,R)-trans	Cis	Cis	(S,S)-trans
TS **D**				
	18	**19**	**20**	**21**
HF/3-21G*	3.2	0.1	0.0	2.0
+ ZPE	3.0	0.0	0.3	2.2
B3LYP/6-31+G*// HF/3-21G*	2.7	0.0	1.4	2.1
TS **A**				
	22	**23**	**24**	**25**
HF/3-21G*	0.0	2.8	6.8	5.4
B3LYP/6-31+G*// HF/3-21G*	0.0	0.8	3.6	4.9
TS **C**				
	26	**27**	**28**	**29**
HF/3-21G*	0.0	2.4	4.1	2.5
+ ZPE	0.0	2.2	4.2	2.3
B3LYP/6-31+G*// HF/3-21G*	0.0	1.3	1.2	1.4

5, **8**, and **10** were substituted with two phenyl groups, and the resulting four stereoisomeric transition structures for each case (**18–29**) were determined (Table 6). Due to CPU limitations, the HF/3-21G* level of theory was used instead of HF/6-31G*. A special technique was used in the case of **22–25**, derived from **8**. As **8** cannot be located as a stationary point at the HF/3-21G* level (see Computational Details), the geometries of **22–25** were determined by freezing the forming C–C bond to 1.853 Å, the value obtained from **17**, and optimizing all other degrees of freedom. Data in Supporting Information suggest that HF/3-21G* produces reasonable values for the other degrees of freedom.

Data in Table 6 can be compared against the experimental result in the catalytic conditions, where stilbene oxide was obtained as a 12:88 cis:trans mixture.[22] Additionally, if steric hindrance is imagined to block one direction of approach, allowing benzaldehyde to approach only from the direction shown in Table 6, Me₂S can be regarded as a very simple model molecule for a chiral sulfide (Scheme 5), allowing comparisons to the experimental enantioselectivities in the catalytic conditions.[4]

The energies are best in line with *trans*-stilbene oxide formation via **22–25** (TS **A**) and **26–29** (TS **C**), not via

(21) The necessary stationary points of the model reaction were redetermined at this lower level of theory for the purpose of concistency.

(22) Aggarwal, V. K.; Abdel-Rahman, H.; Fan, L.; Jones, R. V. H.; Standen, M. C. H. *Chem. Eur. J.* **1996**, *2*, 1024–1030.

Table 7. The Relative Energies (in kcal/mol) and Geometries of the Stereoisomeric C−C Bond Formation Transition States 30−37 (TS A) for Stilbene Oxide Formation. In All Cases the Length of the Forming Bond Was Frozen While All Other Degrees of Freedom Were Optimized. The Four Columns on the Left Correspond to the Approach from the Less-Hindered and the Four on the Right to the Approach from the More-Hindered Side of the Ylide

	(R,R)-trans-**30**	cis-**31**	cis-**32**	(S,S)-trans-**33**	(S,S)-trans-**34**	cis-**35**	cis-**36**[a]	(R,R)-trans-**37**[b]
				Energy				
experimental[c]	0.0	>2.3	>2.3	2.0				
HF/3-21G*	0.0	1.4	5.6	4.3	4.7	4.0	8.9	7.3
B3LYP/6-31+G*//HF/3-21G*	0.0	0.2	3.4	4.1	4.2	2.9	6.0	4.9
				Geometry[d]				
S−C (Å) (2-4)	1.802	1.788	1.783	1.784	1.827	1.807	1.833	1.820
C−C (Å) (4-5)[e]	1.853	1.853	1.853	1.853	1.853	1.853	1.853	1.853
CCO (deg) (4-5-6)	103	104	105	104	103	104	105	107
SCCO (deg) (2-4-5-6)	146	166	−170	−142	−153	−168	−173	−162
CSCC[f] (deg)	−64	−51	−73	−69	93	72	105	81
$CCC_{ar}C_{ar}$[g] ylide (deg)	15	17	25	30	10	16	29	49
$CCC_{ar}C_{ar}$[g] PhCHO (deg)	14	14	6	6	19	15	10	12

[a] Stopped after 49 optimization steps and insignificant residual energy change. [b] After 15 optimization steps; further optimization led to SCCO torsion angle less than 120°. [c] The 93% ee and cis−trans ratio of <2:98 from literature[4] for the reaction illustrated in Scheme 2. Converted to energies using the relationship $\Delta G = -RT \ln K$ at rt. [d] Numbering system from Figure 4. [e] Frozen coordinate. [f] Coordinate definition 1-2-4-5 in **30**−**33** and 3-2-4-5 in **34**−**37**. [g] See Table 4, note b.

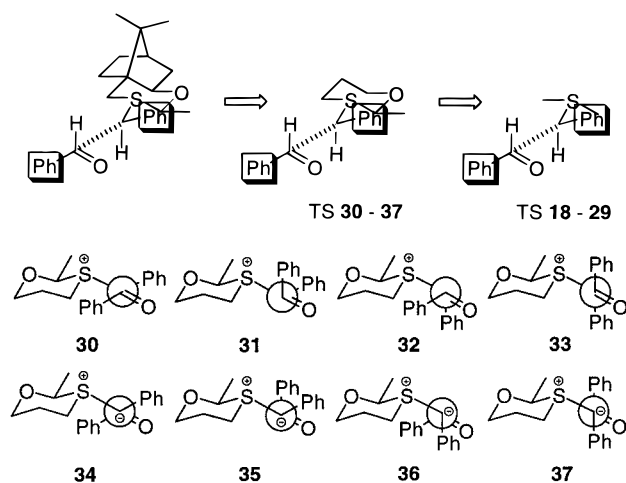**Scheme 5. Simplification of the Sulfide Moiety in the TSs**

TS **30** - **37**   TS **18** - **29**

30   **31**   **32**   **33**

34   **35**   **36**   **37**

Figure 5.

18−21 (TS **D**). Although the trans approach is favored in **18−21**, conversion of the resulting oxathietanes to epoxides via the torsional rotation pathway produces *cis*-stilbene oxide. Additionally, here TSs **A** and **C** but not **D** can account for the formation of (R,R)-*trans*-stilbene oxide. Consequently, further studies were carried out with **A** and **C**, using substituents that allowed more direct comparison with experiment.

The Stereoisomeric C−C Bond Formation Transition States with 14 as the Ylide Component. The data above suggested that transition states **A** or **C** are likely to be responsible for enantioselectivity of *trans*-stilbene oxide formation. First, we carried out more detailed studies with TS **A**. When a sulfonium ylide derived from a chiral sulfide is used in the Corey−Chaykovsky reaction, formation of the three stereoisomers of stilbene oxide can occur through eight stereoisomeric transition states **30−37** (Figure 5). In these transition states, the monocyclic sulfonium benzylide **14** is a model molecule for the tricyclic sulfonium benzylide **15**, allowing comparisons with experimental data (Scheme 5).[4] Additionally, only the equatorial sulfur electron pair is expected to be reactive in the ylide formation from the parent sulfide of **15**.[23]

Due to the large size of **30−37**, HF/6-31G* or HF/3-21+G* were not practical for geometry optimizations. Since lower levels are not able to locate **8** or its derivatives, HF/3-21G* and the freezing strategy discussed above, considered the best compromise between speed and accuracy, were used to determine the geometries of the transition structures **30−37**.[24] The resulting geometries and energies for the transition structures are listed in Table 7, along with the energy values converted from experimental data for comparison. Two of the geometries result from incomplete optimization and are consequently estimates within our protocol. Fortunately, they are the highest energy structures and not decisive in drawing conclusions out of the data set.

Due to freezing, the geometry data should be treated with caution, bearing in mind that the reported coordinates reflect values for all other coordinates at a fixed point along the reaction coordinate. However, the anti conformation in the starting material ylide clearly results in increased $CCC_{ar}C_{ar}$ angles and probably in a reduced conjugative stabilization in all corresponding transition structures. Additionally, the aldehyde approaching from the more-hindered side of the ylide consistently results in increased CSCC angles, measuring the rotation of the reaction coordinate relative to the sulfide moiety.

The relative energies of the transition states qualitatively account for the product distribution. Consequently, the TS for (R,R)-*trans*-stilbene oxide formation is lower in energy than the one for (S,S)-*trans*-stilbene oxide formation (enantioselectivity), and the transition states leading to trans epoxides have a lower energy than those leading to cis epoxides (diastereoselectivity). For enantioselectivity, facial and conformational selectivity seem equally important. The energy trends are similar both at HF/3-21G* and B3LYP/6-31+G*//HF/3-21G* levels, with the lower level providing a better account of experiment. Quantitatively, the theoretical results overestimate enantioselectivity and underestimate diastereoselectivity.

There is an increased preference for the syn ylide conformation in the transition states compared to the ylides themselves, and the transition state model offers

(23) Aggarwal, V. K.; Thompson, A.; Jones, R. V. H.; Standen, M. *Tetrahedron: Asymmetry* **1995**, *6*, 2557−2564.
(24) Several freezing strategies were tested in an effort to use PM3, but this approach was found unreliable.
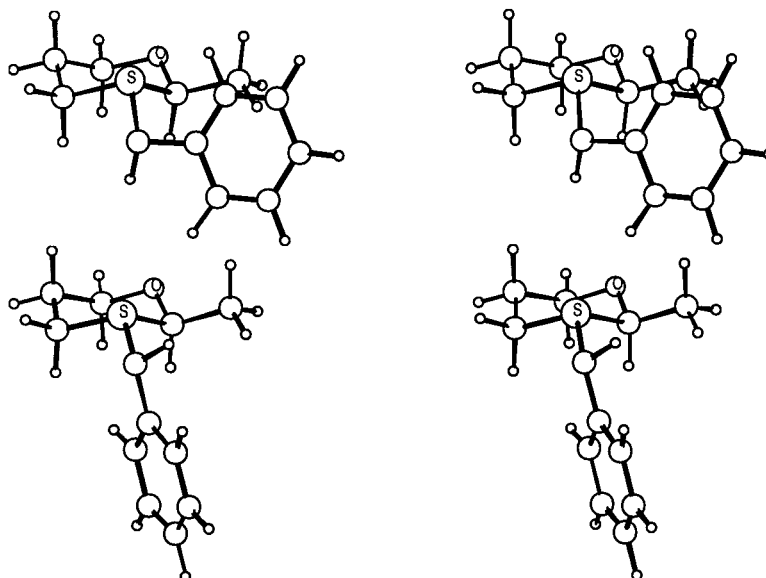
Figure 6. Stereoviews of **30** (top, syn ylide conformation) and **33** (bottom, anti ylide conformation), with the benzaldehyde component removed for clarity. The TSs lead to the formation of (R,R)-*trans*- and (S,S)-*trans*-stilbene oxide, respectively. In the syn TS the shortest interatomic distance between the phenyl group and thioacetal methyl is 2.7 Å. In the anti TS, the shortest distance between the axial hydrogen and phenyl hydrogen is 2.0 Å (2.2 Å in the ylide itself).

Table 8. The Relative Energies (in kcal/mol) and Geometries of the Stereoisomeric Ring Closure Transition States 30′–37′ (TS C) for Stilbene Oxide Formation. The Four Columns on the Left Correspond to the Approach from the Less-Hindered and the Four on the Right to the Approach from the More-Hindered Side of the Ylide

	(R,R)-*trans*-**30′**	*cis*-**31′**	*cis*-**32′**	(S,S)-*trans*-**33′**	(S,S)-*trans*-**34′** [a]	*cis*-**35′**	*cis*-**36′** [a]	(R,R)-*trans*-**37′**
				Energy				
experimental[b]	0.0	>2.3	>2.3	2.0				
HF/3-21G*	0.0	0.7	1.7	0.0	0.8	1.5	4.8	0.3
+ZPE	0.1	0.8	2.1	0.0	NA[g]	1.6	NA	0.3
B3LYP/6-31+G*//HF/3-21G*	1.8	2.5	2.1	2.1	0			
				Geometry[c]				
S–C (Å) (2-4)	2.078	2.086	2.048	2.098	2.081[d]	2.046	2.026[d]	2.036
C–C (Å) (4-5)	1.591	1.563	1.590	1.571	1.567[d]	1.564	1.595[d]	1.568
CCO (deg) (4-5-6)	94	95	99	99	95[d]	96	100[d]	100
SCCO (deg) (2-4-5-6)	159	166	−178	170	−172	−167	170	−174
CSCC[e] (deg)	−72	−52	−94	−73	119	71	117	139
CCC$_{ar}$C$_{ar}$[f] ylide (deg)	4	6	44	74	43	6	36	80
CCC$_{ar}$C$_{ar}$[f] PhCHO (deg)	4	13	16	4	3	14	15	1

[a] Despite several attempts, the transition states could not be located as saddle points. To obtain these estimates, some coordinates were frozen while all others were relaxed. [b] The 93% ee and cis–trans ratio of <2:98 from literature[4] for the reaction illustrated in Scheme 2. Converted to energies using the relationship $\Delta G = -RT \ln K$ at rt. [c] Numbering system from Figure 4. [d] Frozen coordinate. The value was obtained from **26** and **28** for **34′** and **36′**, respectively. [e] Coordinate definition 1-2-4-5 in **30′**–**33′** and 3-2-4-5 in **34′**–**37′**. [f] See Table 4, note *b*. [g] NA = not applicable.

a structural explanation for it. In the TS the ylide carbon becomes pyramidal while the phenyl group prefers to remain conjugated to the anionic ylide carbon. Consequently, the phenyl group bends away from the plane formed by the sulfur lone pair, the sulfur atom itself, and the ylide carbon upon going from the ylide to TS **A**. In syn sulfonium benzylides the close contact between the lone pair of the sulfur atom and one of the hydrogens of the phenyl group is maximal in the ylide itself but is reduced upon going to the TS (Figure 6, top). In anti sulfonium benzylides the close contact between the axial hydrogens and one of the hydrogens of the phenyl group is minimal in the ylide but is increased upon going to the TS, as the phenyl group has to rotate to remain in conjugation (Figure 6, bottom). Due to the difficulty of accommodating the phenyl group, inferior conjugation, as measured by the CCC$_{ar}$C$_{ar}$ torsion angle (Table 7), is observed in the TSs derived from anti sulfonium benzylides. Consequently, steric strain is reduced in syn sulfonium benzylides and increased in anti sulfonium

benzylides upon going from the ylides to the corresponding transition states **A**.

The Stereoisomeric Ring Closure Transition States with 14 as the Ylide Component. The eight stereoisomeric C–C bond formation transition states **30**–**37** have eight closely related transition structures, assigned as **30′**–**37′**, which are substituted versions of **10**. Their geometries were determined at the HF/3-21G* level with optimization to transition states, with two exceptions where freezing of coordinates was necessary. The resulting geometries and the associated energies are listed in Table 8. The main difference in the overall geometries between the corresponding C–C bond formation and ring closure transition states are the CCC$_{ar}$C$_{ar}$ rotation angles in the ylide, in addition to the obvious differences in the coordinates of the reactive center. Apparently, conjugation between the ylide carbon and the aromatic ring is not as important as in the C–C bond formation TS, resulting in more freely adjusting aromatic rings.

The relative energies of the transition states cannot directly account for the experimentally observed product distribution as they did in the C−C bond formation TS **A**. In fact, the more reliable B3LYP/6-31+G* energies predict the formation of the wrong enantiomer of *trans*-stilbene oxide due to a preference of the more-hindered face of the ylide. The cis/trans selectivity is somewhat but not significantly better reproduced than in the C−C bond formation TS. ZPE contributions are small, as expected for a stereoisomeric series. The coordinates for **30**−**37** and **30′**−**37′** are available from the authors upon request.

Discussion

Ylide Conformational Preference. In the reaction of **15** with benzaldehyde under catalytic conditions, Aggarwal et al. rationalize the preferential formation of (*R*,*R*)-*trans*-stilbene oxide over the (*S*,*S*)-trans isomer as resulting from the absolute stereochemistry of the parent sulfide of **15** and the less-hindered direction of approach of benzaldehyde (Scheme 2), while assuming that the syn ylide conformer is favored over the anti in **15**. The anti conformer is expected to suffer from 1,3-diaxial interactions of the phenyl group with the axial hydrogens, thus leading to the preference for the syn conformer. Unfortunately, efforts toward experimental conformational analysis by NMR have failed so far because of the rearrangement of sulfonium benzylides.[17] Due to the central role of the syn vs anti conformational preference in **15**, we estimated the relative energies of the conformers theoretically.

CPU limitations prevented us from directly estimating the geometries and relative energies of the two conformers of **15** at a high level of theory in CH_2Cl_2. However, a series of three systems, **13**−**15**, provided us an extrapolated estimate for the conformational preference and also allowed us to estimate the sensitivity of the results to the level of theory. In a model system, estimates from different modeling approaches treat the ylide conformational preference relatively unanimously, suggesting that this property can be modeled relative reliably, at least in the gas phase. Overall, the sulfonium benzylide conformational preference seems small, and extrapolation of our results to **15** suggests a preference of 0.8 kcal/mol for the anti conformer in CH_2Cl_2. The experimentally observed 93% ee would correspond to 2.0 kcal/mol syn preference, implying that the ylide conformational preference *in the ground state* does not account for the observed stereoselectivity. This is unfortunate from the perspective of molecular design, as the ylide conformational preference is simple and quick to model, compared to the transition state calculations that proved necessary.

The Reaction Pathways. Although the concerted pathway has been demonstrated experimentally, most accounts of stereoselective Corey−Chaykovsky reactions rationalize the product distribution by utilizing an anti addition or head to tail addition model similar to TS **A**. Our results with the model reaction suggest that the anti addition and torsional rotation pathways are favored over the concerted pathway by at least 10 kcal/mol, with CH_2Cl_2 solvation increasing the preference. However, it is more difficult to predict whether the anti addition or torsional rotation pathway or both operate in a particular case, with a particular combination of substituents and reaction conditions.

In the model reaction both pathways are energetically feasible. Since a substituted version of **4** has been isolated and characterized by X-ray,[25] oxathietanes similar to **4** have been proposed to be intermediates in the Corey−Chaykovsky reaction. While previous modeling studies indicated that there is no barrier for the addition leading to oxathietane similar to **4**,[7] we were able to locate **5** as a transition state for this type of addition. Thus, the pathway adopted by the model reaction depends on the relative energies of **5** and **8**. In the gas phase, **5** is favored over **8**, but higher activation energies are required to convert **4** to the products via torsion rotation or concerted mechanism than dissociation of **4** back to the starting materials and recombination via the anti addition pathway and reaction to the products. In CH_2Cl_2 **8** is energetically favored over **5**, but the difference is very small, less than 1 kcal/mol.[26] Furthermore, the torsion rotation pathway, reached via **5**, also becomes energetically accessible in solution. Thus, in the model reaction, both the anti addition pathway and the torsion rotation pathway appear to operate in solution. In the context of stilbene oxide formation in the catalytic conditions, we favor the anti addition pathway for reasons discussed below.

As noted in Results, the apparent lack of energy barriers in the initial combination of the starting materials (Figure 3) is specific to the model reaction and is probably caused by our modeling protocol. Similar behavior has been observed in a computational study with ylides of N, P, As, Sb, and Bi, where weak starting material complexes could be located as shallow minima and, consequently, TSs closely related to **5** and **8** represented small energy barriers.[27] We assume our model reaction represents an analogous case. Additionally, the nature of **6** as a hot nucleophile with a pyramidal, anionic ylide carbon is likely to contribute to the low energy barriers in the gas phase.[28] The energies in solution, in turn, are affected by the lack of relaxation in the presence of solvent, which might have changed the relative energies of the stationary points. In any case, our modeling approach yields an energy barrier for product formation both in the gas phase and in solution with sulfonium benzylides. Overall, phenyl substitution increases the activation energy and lowers the reaction energy.

The Effect of the Reaction Medium on the Mechanism. In the model reaction, CH_2Cl_2 solvation *selectively* lowers the energies of the polar stationary points **8**−**12**, favoring the polar anti addition and torsional rotation pathways. Furthermore, according to our calculations, **9** and **10**, not found in the gas phase at the B3LYP/6-31+G* level, are likely to be stationary points in solution also at this level of theory.[29] Consequently, the reaction medium may have a significant effect on the reaction mechanism of the Corey−Chaykovsky reaction. Previous theoretical calculations have been unable to locate **B** and **C**, probably because they are highly polar, and solvents

(25) Ohno, F.; Kawashima, T.; Okazaki, R. *J. Am. Chem. Soc.* **1996**, *118*, 697−698.

(26) However, the solvation effect is 9 kcal/mol for **8** and 3 kcal/mol for **5**, suggesting that **8** could be even more favored if optimization in solution had been available.

(27) Naito, T.; Nagase, S.; Yamataka, H. *J. Am. Chem. Soc.* **1994**, *116*, 10080−10088.

(28) A counterion would probably be present in typical applications of sulfonium methylides, lowering the energy of the starting materials.

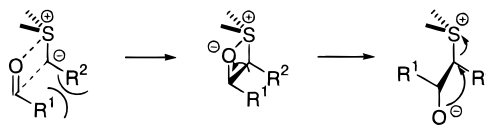(29) They are stationary points at the HF/6-31G* level, as discussed in Results.

stabilize structures with high dipole moments. Since CH_2Cl_2 is relatively nonpolar, the relative energies and possibly also the geometries of **8**−**12** can be expected to be very sensitive to different solvents. While only single point calculations in CH_2Cl_2 were possible to us at the time of writing, relaxation in the presence of solvent might have revealed **9** as a deeper minimum and probably would have affected all SCCO torsion angles reported in this study.

While sensitive to solvation, **A**, **B**, **C**, and **F** can be expected to be even more sensitive to coordinating counterions, such as lithium and sodium. In their studies of the concerted pathway in a salt-free medium, Kawashima et al. observed that the addition of lithium salts reduced the stereoselectivity, concluding that salt-free Corey−Chaykovsky reactions proceed via the concerted pathway.[3] However, the substituents and the oxidation state of sulfur were different from those typically employed in the catalytic Corey−Chaykovsky reaction. Furthermore, our computational studies with the model reaction naturally represent salt-free conditions and suggest that also the salt-free Corey−Chaykovsky reactions can preferentially proceed via the other two pathways, torsion rotation and anti addition. Of the latter two, the anti addition pathway is probably more favored by counterions, as coordination of a counterion to the aldehyde oxygen is expected to be more favorable in the case of **A** than in **D**.

The exact sequence of steps on the anti addition pathway is likely to be affected by coordinating counterions, as the counterions are likely to change the relative energies of **B** and **C** more than that of **A**. In the presence of salts, **B** may be a true intermediate and two consecutive transition states, **A** and **C**, may be involved. Experimentally, a two-transition state mechanism has been proposed in a Corey−Chaykovsky variant where β-hydroxy sulfonium salts have been treated with NaOH.[30] However, the reaction medium employed in the catalytic conditions contains either $Rh_2(OAc)_4$ or $Cu(acac)_2$ dissolved in CH_2Cl_2, both weaker in their coordinating power than lithium or sodium salts and present in only catalytic quantities. Consequently, in the catalytic conditions the involvement of **B** and **C** is more difficult to anticipate. It could vary from case to case, depending on the exact conditions and substituents, as in the model reaction **B** appears to be a very shallow minimum.[31] However, it should be noted that the configuration of stereocenters is determined in **A**, both when product formation occurs directly or via **B** and **C**.

Which Transition State Determines Stereoselectivity? Experimental evidence suggests that the additions of sulfonium benzylides to carbonyl compounds are under kinetic control.[30] According to NMR data, the

(30) Aggarwal, V. K.; Calamai, S.; Ford, J. G. *J. Chem. Soc., Perkin Trans. 2* **1997**, 593−599.

(31) Attempts to locate substituted version of **B** corresponding to *trans*-stilbene oxide formation at the HF/6-31G* level of theory were unsuccessful.

(32) The $CCC_{ar}C_{ar}$ (ylide) torsional angle is defined by the carbon atoms in dark.

Scheme 6. Formation of Trans Epoxides via the Torsional Rotation Pathway

barrier of rotation about the ylide bond in dimethylsulfonium fluoren-9-ide is 10 kcal/mol, a facile process at room temperature.[17] Assuming a rotational barrier of similar magnitude in **15**, the Curtin−Hammett principle applies, and the product distribution is determined by the relative energies of the transition states only.

Excluding the concerted transition state **G** due to its high energy in the model reaction, the configuration of stereocenters is fixed in two different types of transition states, **A** and **D**. While reactions proceed via low energy transition states, data from the simple model reaction with **5** and **8** themselves do not allow us to identify the more probable pathway in the case of substituted systems. However, the torsional rotation pathway has difficulties in accounting for the preferential formation of trans epoxides observed in practically all reported Corey−Chaykovsky reactions. Since in this scenario the stereochemistry is determined in TS **D**, the trans geometry of the resulting epoxide is fixed in a sterically congested form of the TS (Scheme 6). Thus, it appears that at least trans epoxides might be preferentially formed via TS **A**.

Our computational data with substituted transition states **18**−**29** in the context of stilbene oxide formation (Table 6) support the previous intuitive conclusion. Even though some transition states are approximated by the freezing strategy, it should be noted that comparisons within a stereoisomeric transition state series benefit from maximal cancelation of errors. The relative energies of the stereoisomeric transition states are in line with *trans*-stilbene oxide formation via the anti addition pathway, with involvement of TS **A** (and **D**). Furthermore, CH_2Cl_2 solvation is likely to further increase the energy differences between the cis and trans transition structures to favor trans geometries, which would further support the conclusion.

As TSs **A** (and **D**) were implicated in the determination of stereoselectivity by the considerations outlined above, these types of transition states were further studied computationally in systems allowing comparison with experimental enantioselectivity data of stilbene oxide formation.
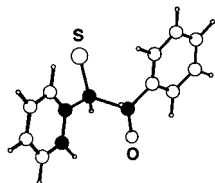
The Stereoisomeric Transition States 30−37. We studied the addition of **14** to benzaldehyde by determining the corresponding substituted versions of **A** and **D**. These transition states are models for the addition of **15** to benzaldehyde, for which experimental data under catalytic conditions are available.[4] The relative energies of the eight stereoisomeric C−C bond formation transition states **30**−**37** (TS **A**) qualitatively account for the experimentally observed product stereoisomer distribution whereas the corresponding series of ring closure transition states **30′**−**37′** (TS **D**) does not.

Even though a fully quantitative agreement with experiment was not achieved, our data provide additional insights into the origins of the stereoselectivity in the Corey−Chaykovsky reaction. Our results suggest that the ylide conformational preference and direction of

aldehyde approach are equally important in determining the enantioselectivity. The ability to computationally distinguish between the two contributions to enantioselectivity is important in designing new sulfides for this reaction.

In comparing theory and experiment, we have assumed that only one of the sulfur electron pairs is reactive. If the more-hindered electron pair had any residual reactivity leading to opposite enantioselectivity, lower overall % ee would be observed compared to the maximal value predicted by the series **30**−**37**.

Methodological Issues. The energies of the stereoisomeric C−C bond formation TSs, although in qualitative agreement with experiment, do not provide an accurate quantitative account. From the computational viewpoint this is understandable, since **30**−**37** are pseudo-transition states obtained by frozen optimizations. However, while absolute activation energies are difficult to calculate correctly, predictions of relative activation energies are usually much more successful, as they benefit from cancelation of errors, such as systematic errors in theoretical treatment and systematic solvent, counterion, and other medium effects. Maximal cancelation of errors can be expected in the case of stereoisomers, such as **30**−**37**, probably responsible for the success in the qualitative prediction.

From the methodological viewpoint, we would have benefited from a practical method allowing geometry optimizations in solution. Even though dichloromethane is not a highly polar solvent, it has a significant effect on the energies of highly polar structures. Due to the anti orientation of sulfur and oxygen with high positive and negative partial charges, respectively, the anti addition pathway consists of structures with a very high dipole moment. In some cases with the frozen C−C bond formation, transition state optimizations resulted in SCCO torsion angles less than 120° even if the optimization were started with SCCO value close to 180°. This may have been due to the overestimation of Coulombic attraction in the gas phase whereas optimization in dichloromethane might have stabilized the anti orientation sufficiently to allow complete optimization.

Conclusions

We have compared reaction pathways of the Corey−Chaykovsky epoxidation reaction constructed from previous literature proposals and data obtained here. Of the concerted, anti addition and torsional rotation pathways, the anti addition pathway has been previously used to rationalize the stereoselectivity of the catalytic Corey−Chaykovsky reaction, carried out in CH_2Cl_2.[4] Our quantum chemical studies of the reaction revealed five new intermediates and transition states not previously characterized theoretically. Additionally, the reaction appears to be sensitive to solvent and other reaction medium effects. According to computational studies with a model reaction, the anti addition and torsional rotation pathways are favored over the concerted one by at least 10 kcal/mol, and the preference is further enhanced in CH_2Cl_2. Although in the model reaction the torsional rotation and anti addition pathways are equally accessible, trans epoxides are probably formed via the anti addition pathway. Our computational results obtained from substituted systems suggests that at least stilbene oxide forms via the anti addition pathway.

Furthermore, TS **A**, suitably substituted to allow comparison with experiment (TSs **30**−**37**), is able to predict both the absolute stereochemistry of the main product and, qualitatively, the distribution of its other stereoisomers, supporting the published rationalization.[4] *Our theoretical results are, therefore, consistent with the carbon−carbon bond formation transition state **A** being responsible for the stereoselectivity of trans-stilbene oxide formation in the catalytic Corey−Chaykovsky reaction.* The results support the commonly used anti addition model and show how the syn sulfonium benzylide is preferred over the anti in the transition state rather than in the ground state.

Overall, we have been able to clarify the origins of stereoselectivity in the catalytic version of the Corey−Chaykovsky reaction and have validated a practical quantum chemical protocol for predicting the stereoselectivity. The protocol is useful in designing new sulfides for the reaction, allowing conformational and directional contribution to enantioselectivity to be estimated separately. The modeling approach helped us in designing novel, highly enantioselective catalysts for the Corey−Chaykovsky reaction, and their structures, preparation, and evaluation will be reported in due course.

Supporting Information Available: Conformational energy difference of **13** at various levels of theory; comparison of geometry parameters of **17** from two optimizations at two levels of theory and selected stationary points, energies, zero-point energies, and Cartesian coordinates. This material is available free of charge via the Internet at http://pubs.acs.org.

JO9818935